Clinical Cancer Research

Aberrant Lck Signal via CD28 Costimulation Augments Antigen-Specific Functionality and Tumor Control by Redirected T Cells with PD-1 Blockade in Humanized Mice

Pratiksha Gulati[1,2], Julia Rühl[2], Abhilash Kannan[3], Magdalena Pircher[1], Petra Schuberth[1], Katarzyna J. Nytko[4], Martin Pruschy[4], Simon Sulser[5], Mark Haefner[6], Shawn Jensen[7], Alex Soltermann[8], Wolfgang Jungraithmayr[9,10], Maya Eisenring[11], Thomas Winder[1], Panagiotis Samaras[1], Annett Tabor[12], Rene Stenger[13], Roger Stupp[1], Walter Weder[9], Christoph Renner[14], Christian Münz[2], and Ulf Petrausch[1,2,15]

Abstract

Purpose: Combination therapy of adoptively transferred redirected T cells and checkpoint inhibitors aims for higher response rates in tumors poorly responsive to immunotherapy like malignant pleural mesothelioma (MPM). Only most recently the issue of an optimally active chimeric antigen receptor (CAR) and the combination with checkpoint inhibitors is starting to be addressed.

Experimental Design: Fibroblast activation protein (FAP)–specific CARs with different costimulatory domains, including CD28, Δ-CD28 (lacking lck binding moiety), or 4-1BB were established. CAR-T cells were characterized *in vitro* and antitumor efficacy was tested *in vivo* in a humanized mouse model in combination with PD-1 blockade. Finally, the Δ-CD28 CAR was tested clinically in a patient with MPM.

Results: All the three CARs demonstrated FAP-specific functionality *in vitro*. Gene expression data indicated a distinct activity profile for the Δ-CD28 CAR, including higher expression of genes involved in cell division, glycolysis, fatty acid oxidation, and oxidative phosphorylation. *In vivo*, only T cells expressing the Δ-CD28 CAR in combination with PD-1 blockade controlled tumor growth. When injected into the pleural effusion of a patient with MPM, the Δ-CD28 CAR could be detected for up to 21 days and showed functionality.

Conclusions: Overall, anti-FAP-Δ-CD28/CD3ζ CAR T cells revealed superior *in vitro* functionality, better tumor control in combination with PD-1 blockade in humanized mice, and persistence up to 21 days in a patient with MPM. Therefore, further clinical investigation of this optimized CAR is warranted. *Clin Cancer Res; 24(16); 3981–93. ©2018 AACR.*

[1]Department of Oncology, University Hospital Zurich, Zurich, Switzerland. [2]Institute for Experimental Immunology, University of Zurich, Zurich, Switzerland. [3]Institute of Molecular Life Sciences, University of Zurich, Zurich, Switzerland. [4]Department of Radiation Oncology, University Hospital Zurich, Zurich, Switzerland. [5]Institute of Anesthesiology, University Hospital Zurich, Zurich, Switzerland. [6]Oncology Bülach, Bülach, Switzerland. [7]Laboratory of Molecular and Tumor Immunology, Earle A. Chiles Research Institute, Providence Cancer Center and Providence Portland Medical Center, Portland, Oregon. [8]Institute of Pathology and Molecular Pathology, University Hospital Zurich, Zurich, Switzerland. [9]Department of Thoracic Surgery, University Hospital Zurich, Zurich, Switzerland. [10]Department of Thoracic Surgery, Campus Ruppiner Kliniken, Medical University Brandenburg, Brandenburg, Germany. [11]Department of Immunology, University Hospital Zurich, Zurich, Switzerland. [12]European Institute for Research and Development of Transplantation Strategies GmbH (EUFETS), Idar-Oberstein, Germany. [13]Swiss Center for Regenerative Medicine, Wyss Institute, University of Zurich, Zurich, Switzerland. [14]Department of Biomedicine, University Hospital Basel, Basel, Switzerland. [15]Swiss Tumor Immunology Institute, Zurich, Switzerland.

Note: Supplementary data for this article are available at Clinical Cancer Research Online (http://clincancerres.aacrjournals.org/).

C. Münz and U. Petrausch contributed equally to this article.

Corresponding Author: Ulf Petrausch, University of Zurich, 8057 Zurich, Switzerland. Phone: 41-44-635-37-01; E-mail: ulf.petrausch@uzh.ch

doi: 10.1158/1078-0432.CCR-17-1788

©2018 American Association for Cancer Research.

Introduction

Chimeric antigen receptors (CARs) are composed of an antibody-derived, target antigen-specific single-chain variable fragment (scFv) which is linked to T-cell costimulatory domains such as CD28, 4-1BB, ICOS, CD27, or OX40, in addition to the T-cell signaling domain CD3ζ (1). CARs can be designed to recognize tumor-associated antigens (TAA) and thereby can be utilized to redirect T cells against cancer cells.

Until now, most remarkable clinical responses have been observed using anti-CD19-CARs in hematologic malignancies (2). Based on these promising results, redirected T-cell therapy needs further evaluation, to allow for clinical benefit in other malignancies, especially solid tumors.

Preclinical evaluation of redirected T cells often uses immune-compromised mouse models. These models provide limited understanding of the interplay between human tumors and redirected T cells, without depicting interactions with other immune system components. Unlike in a human host, the transferred T cells cannot benefit from human cytokines such as IL7 and IL15 (3). Furthermore, in immune-compromised mice, adoptive transfer of T cells educated outside the mouse host can result in graft-versus-host-disease (GvHD; ref. 3). Humanized mouse models overcome some of these limitations and have

Downloaded from http://aacrjournals.org/clincancerres/article-pdf/24/16/3981/2045305/3981.pdf by guest on 27 August 2022

Translational Relevance

One of the most pressing obstacles for immunotherapy for cancer is the development of rational based combination therapies because monotherapies only allow responses in a limited patient population. Herein, we demonstrated the bench-to-bedside development of fibroblast activation protein (FAP)-specific CAR-redirected T cells. For optimal testing of redirected T cells, a humanized mouse model containing most components of the human immune system was developed. CARs with distinct costimulatory domains were designed and tested. We identified a particular CAR with a mutated CD28 signaling domain that provided enhanced antigen-specific proliferation, increased T-cell metabolism, activation and redirected T cell mediated tumor control in combination with PD-1 blockade *in vivo*. Additionally, we used these data to launch a first-in-man clinical trial injecting FAP-specific redirected T cells in the pleural effusion of patients with malignant pleural mesothelioma. Our preclinical and clinical data lay the groundwork for further testing of FAP-specific redirected T cells.

demonstrated to be a powerful model system at least for the study of human viruses (4). Using human hematopoietic progenitor cells (HPC), immune-compromised mice develop most human lymphocyte and myeloid lineages (5). Attributed to the partly developed human immune environment, humanized mice can provide a robust host, for blocking or boosting anticancer immune reactions mediated by adoptively transferred redirected T cells.

Malignant pleural mesothelioma (MPM) is a disease that cannot be cured even at early stages (6). Recently, encouraging data using PD-1–blocking antibodies indicated that the immune system can attack MPM and result in clinical responses (7, 8). However, only a minority of patients responded to PD-1 blockade. One possible explanation could be the absence of a T-cell repertoire that can generate a therapeutic immune response. A potential approach to overcome this limitation is transfer of redirected T cells recognizing antigens expressed in MPM. Fibroblast activation protein (FAP) is expressed in MPM and is therefore a potential target antigen (9). We constructed anti-FAP (scFv F19) CAR constructs with different costimulatory moieties, CD28, Δ-CD28, and 4-1BB and tested them *in vitro* and in a humanized mouse model. The Δ-CD28 CAR carries a deletion in the lck binding domain, which was initially shown to augment antitumor responses due to aberrant IL2 production, which was no longer available to sustain persistence of Tregs, infiltrating tumors (10).

Our data indicate that the Δ-CD28 CAR mediates superior *in vitro* functionality, showed enhanced metabolism, activation after cognate antigen encounter, and mediated better tumor control in combination with PD-1 blockade in humanized mice. Based on these findings, the Δ-CD28 CAR was further used for a first-in-man adoptive transfer of FAP-specific redirected T cells in patients with MPM. This study provides the rationale for further exploring FAP-specific Δ-CD28 CAR-redirected T cells in patients with MPM and other malignant tumors expressing FAP.

Materials and Methods

Cell lines

293T cells were purchased from ATCC. HT1080FAP and HT1080PA cell lines were generated by stably transfecting HT1080 cells with human FAP or mock plasmid, respectively, in addition to the luciferase plasmid, as described previously (11). All cell lines were routinely tested and confirmed negative for *mycoplasma* contamination. For details about culturing conditions, refer to Supplementary Notes.

T-cell activation with anti-CD3/CD28

$CD3^+$ T cells isolated from healthy leucocyte concentrate donors were incubated with CD3/28 beads at 1:5 bead:cell ratio or anti-CD3 and anti-CD28 antibodies (1 μg/mL) either supplemented in T-cell medium [TCM; RPMI + 2 mmol/L L-glutamine + 10% FBS + 50 U/mL penicillin + 50 μg/mL streptomycin and 1× NEAA (nonessential amino acids solution)] or coated on 24 well plates (Corning). After 48 hours, the CD3/28 stimulus was removed and cells were incubated in TCM supplemented with 200 IU/mL IL2 (Peprotech), and 10 ng/mL of both IL7 and IL15 (Miltenyi Biotech). Alternatively, cells were labeled with carboxyfluorescein succinimidyl ester (CFSE) and CFSE dilution assays were performed as described before (12). Phenotypic markers were analyzed by flow cytometry at several time points after removal of the CD3/28 stimulus.

Generation of CAR constructs and retroviral transduction of T cells

The scFv of the FAP-specific CAR (F19; ref. 11) and the NY-ESO-1–specific CAR (T1), which serves as control in this study (recognizing the HLA-A*02:01/NY-ESO-$1_{157\text{-}165}$ peptide complex; ref. 13) flanked by NCOI and BamHI restriction sites, was cloned into the pBullet vector (14), containing a human Δ-CH2/CH3 domain of the costimulatory domains of either CD28, Δ-CD28, or 4-1BB, and the CD3ζ domain (kindly provided by Dr. Hinrich Abken, University of Cologne, Germany). The human Δ-CH2/CH3 domain contains a modification that reduces binding of the respective CARs to $Fc\gamma R^+$ cells (15) and thereby minimizes off-target activation. The Δ-CD28 is a modification of the CD28 costimulatory domain (generated by site directed mutagenesis), which is devoid of the lck kinase binding site (10). The resulting CAR constructs were termed: FAP-specific: F19-CD28/CD3ζ, F19-Δ-CD28/CD3ζ, or F19-4-1BB/CD3ζ; and NY-ESO-1-specific: T1-CD28/CD3ζ, T1-Δ-CD28/CD3ζ, or T1-4-1BB/CD3ζ. Retroviral transduction of human peripheral $CD3^+$ T cells was performed as previously described (13). Cells were cultured in TCM with 200 IU/mL IL2 (Peprotech), 10 ng/mL of both IL7 and IL15 (Miltenyi Biotech). After transduction, CAR-T cells were rested for 4 days in culture before use in an assay.

Flow cytometry

Staining for cell surface markers was carried out by incubating with antibodies for 30 minutes on ice. For intracellular staining, the fixation and permeabilization kit from eBioscience was used, as per manufacturer's instructions. All samples were stained with viability dye to exclude dead cells. The samples were measured on a FACSCanto II or LSRFortessa cytometer (BD Biosciences). Data were analyzed using FlowJo software (TreeStar). For details about staining antibodies, refer to Supplementary Notes.

Downloaded from http://aacrjournals.org/clincancerres/article-pdf/24/16/3981/2045305/3981.pdf by guest on 27 August 2022

In vitro functional assays

Cytotoxicity assays were performed as previously described (16) and as outlined in the Supplementary Notes.

T-cell proliferation was determined *in vitro* using bromodeoxyuridine (BrdU) APC flow kit (BD Biosciences). Briefly, CAR-T cells were seeded on FAP (R&D Systems) coated (2 μg/mL) cell culture plates (Thermo Fisher Scientific) and incubated at 37°C with 5% CO_2 for 72 hours followed by the addition of BrdU (10 μmol/L) and incubation for another 72 hours. The cells were harvested, and staining for BrdU was performed as per the manufacturer's instructions followed by analysis in a flow cytometer.

To analyze cytokine release, supernatants of cocultivated effector and target cells were collected after 12 hours of incubation. IFNγ and IL2 levels were detected using BD OptEIA human IFNγ and human IL2 ELISA kits, respectively, according to the manufacturer's instructions (BD Biosciences). Cytokines IL2, IL6, IL10, IFNγ, and TNFα from human samples were measured using a multiplexed particle-based flow cytometric cytokine assay using cytokine Luminex kits (R&D Systems; ref. 17).

RNA sequencing

$CD8^+$ T cells isolated from three buffy donors ($N = 3$) using CD8 microbeads (Miltenyi Biotech) were transduced to express F19-CD28/CD3ζ, F19-Δ-CD28/CD3ζ, F19-4-1BB/CD3ζ, T1-CD28/CD3ζ, T1-Δ-CD28/CD3ζ, or T1-4-1BB/CD3ζ CARs. After transduction, cells were stimulated with recombinant human FAP for 6 days, and CAR^+ T cells were flow sorted on an FACS Aria III cell sorter (BD Biosciences). Average 1×10^6 sorted CAR^+CD8^+ cells with purity >95% were used for RNA extraction using Quick-RNA MicroPrep kits (Zymo Research) as per the manufacturer's instructions. RNA sequencing was performed at the Functional Genomics Center Zurich (FGCZ) and data analyzed using Bioconductor edgeR software package. For detailed description of RNA sequencing methods and analysis, refer to Supplementary Notes. To validate sequencing data, redirected T cells produced from healthy donors were stimulated with recombinant human FAP for 6 days, and expression of phenotypic markers was analyzed by flow cytometry.

Humanized mice and adoptive T-cell transfer

Human fetal livers (HFLs) were obtained from Advanced Bioscience Resources (Alameda). Leukapheresis products were left over from patients who initially were allocated autologous $CD34^+$ transplantation but did not need further treatment (Department of Oncology, University Hospital Zurich, Switzerland). Isolation of $CD34^+$ cells was performed as per the established protocol (18) and using CD34 microbeads (Miltenyi Biotech) as per the manufacturer's instructions. Purity of CD34 fraction was assessed by FACS, and the cells were cryopreserved (RPMI + 7.5% DMSO + 20% FBS). NOD-*scid IL2Rγ*^{null} (NSG) mice were obtained from The Jackson Laboratory, and bred and raised under specific pathogen-free conditions at the Biologisches Zentrallabor (BZL), University Hospital Zurich, Switzerland. For humanization, newborn NSG mice received 2×10^5 or 2×10^6 $CD34^+$ obtained from HFL or leukapheresis, respectively, as per protocol described previously (19) and in Supplementary Fig. S4A.

To test survival of redirected T cells, FAP-specific 0.2×10^6 CAR^+CD3^+ cells produced from harvested splenocytes of donor huNSG mice, were intravenously injected into recipient huNSG mice (reconstituted with same $CD34^+$ HPCs as donor huNSG mice). Persistence of redirected T cells in the blood or abdominal organs (at the time of sacrifice) was measured by qPCR. To test the antitumor efficacy of redirected T cells, luciferase expressing HT1080FAP tumor cells (0.1×10^6 cells per mouse) were injected intraperitoneally (i.p.) in huNSG. Tumor development was measured by *in vivo* bioluminescence imaging using IVIS 200 Caliper (Caliper Life Sciences) as described previously (11) and based on the tumor burden at day 1, mice were equally distributed in groups. This was followed by adoptive transfer of redirected T cells i.p. at effector/target (E:T) ratio of 4:1 to 8:1. In addition to this, mice were injected i.p. with PD-1–blocking antibody (200 μg per mouse), every fourth day. Tumor volume was measured by bioluminescence as Total Flux (photons/second) and quantified for each animal using software Living Image 3.2 (Caliper Life Sciences) as described previously (11). Mice were regularly monitored and euthanized when the change in body weight exceeded 15% or when they displayed persistent discomfort or deviations from normal behavior.

Quantitative PCR to detect redirected T cells

Cellular DNA was extracted using DNeasy blood and tissue kit (Qiagen). CAR DNA was quantified by real-time PCR using primers Fwd 5′-GAAGATGAGCTGCAAGACCA-3′; Rev 5′-GCCCTTGAACTTCTGGTTGT-3′; Probe 5′-(6FAM)-GTACAC-CATCCACTGGGTCC-(TAMRA)-3′ and Taqman Universal PCR Master Mix (Applied Biosystems). The samples were measured in a CFX384 Touch Real-Time PCR Detection System (Bio-Rad). All samples were tested at least in triplicates.

Study approval and clinical trial

All animal experiments were performed in accordance with the Swiss federal and cantonal laws on animal protection (KEK-ZH-Nr. 2011-0498, KVET 10/2013 and 41/2016). The clinical trial was approved by the cantonal ethics committee of Zürich, Switzerland (ethical committee KEK-ZH-Nr. 2012-0106, registered under NCT01722149). Informed consent was obtained from the trial subject, and the trial was conducted in accordance with the principles enunciated in the current version of the Declaration of Helsinki (DoH), the Essentials of Good Epidemiological Practice issued by Public Health Schweiz (EGEP), the Swiss Law and Swiss regulatory authority's requirements as applicable. The clinical trial for the complete recruitment is still ongoing. No primary endpoints are reported here. For details on clinical trial design, refer to Supplementary Notes.

Results

Stimulation with anti-CD3/CD28 coated beads leads to enhanced activation and reduced expression of senescence marker The ability to expand tumor-specific T cells without impairing their functional capacity is crucial for the success of adoptive immunotherapies in cancer. We investigated the consequences of anti-CD3 and anti-CD28 (CD3/28) stimulation provided by beads or antibodies (either in suspension or plate coated), on the proliferation, phenotype of T cells and their ability to get transduced to express CARs. T cells stimulated with CD3/28 beads or antibodies were monitored for several phenotypic markers at different time points (days 0, 3, 5, 7, and 10) after removal of CD3/28 stimulus (Fig. 1A). CD3/28 bead stimulation led to increased T-cell activation over CD3/28 antibodies, as indicated by significantly

Downloaded from http://aacrjournals.org/clincancerres/article-pdf/24/16/3981/2045305/3981.pdf by guest on 27 August 2022

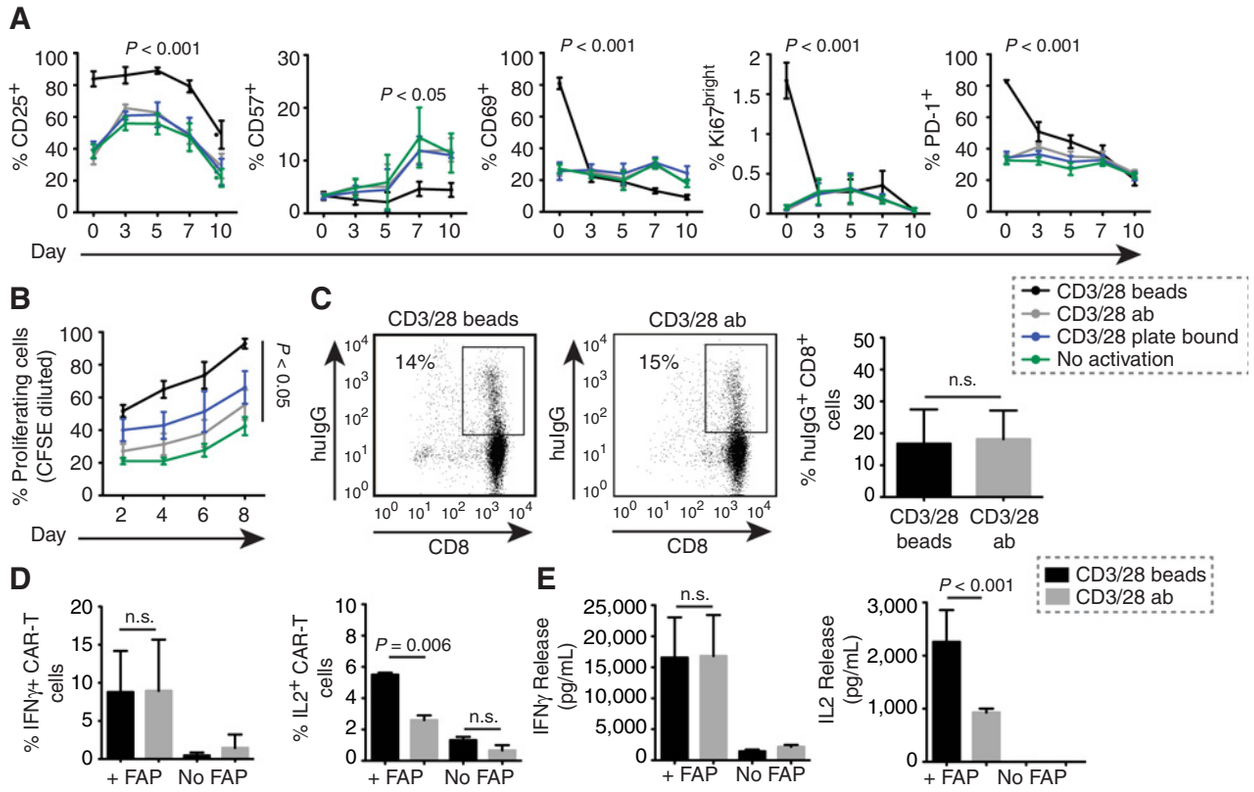

Figure 1.

Phenotypic profiling of T cells activated with CD3/28 beads or CD3/28 antibodies and comparison of transduction efficacies. $CD3^+$ T cells isolated from buffy donors are incubated with anti-CD3 and anti-CD28 coated beads (CD3/28 beads) or anti-CD3 and anti-CD28 antibodies either supplemented in medium (CD3/28 ab) or plate bound (CD3/28 plate bound). **A,** Frequency (%) of $CD25^+$, $CD57^+$, $CD69^+$, $Ki67^{bright}$, and $PD\text{-}1^+$ T cells are compared at days 0, 3, 5, 7, and 10 after removal of CD3/28 stimulus. Pooled data from four leucocyte concentrate donors are shown ($n = 2$). **B,** After removal of CD3/28 stimulus, T cells are CFSE-labeled and frequency (%) of proliferating cells is measured at days 2, 4, 6, and 8. **C,** CD3/28 ab or CD3/28 beads stimulated cells are transduced to express CD28-CD3ζ or Δ-CD28/CD3ζ CARs. Left, Representative FACS plots showing transduction efficacies after CD3/28 beads or CD3/28 ab stimulation. CAR-T cells are detected using antihuman IgG antibody to stain for CAR receptor; gated $huIgG^+CD8^+$ (14% in CD3/28 beads and 15% in CD3/28 ab stimulated T cells). Transduction efficacies after CD3/28 beads or CD3/28 ab activation are compared (right; $n = 4$). **D,** $CD8^+$ cells activated with CD3/28 beads or CD3/28 ab are transduced to express F19-CD28/CD3ζ CAR. Frequency (%) of $IFN\gamma^+$ and $IL2^+$ CAR-T cells (by intracellular staining) and total IFNγ and IL2 production (by ELISA; **E**) is compared in response to antigen-specific (+FAP) stimulation or no stimulation (no FAP). Representative data from one experiment with two buffy donors are shown ($n = 2$). Statistics is done using unpaired *t* test. Data, mean ± SEM.

higher frequencies of $CD25^+$ cells. Additionally, frequency of $CD69^+$ (early marker of T cell activation), $PD\text{-}1^+$ and $Ki67^{bright}$ (proliferation marker) cells, was significantly higher in CD3/28 beads stimulated cells, immediately after removal of stimulus (day 0). In contrast, frequency of $CD57^+$ cells, indicating replicative senescence (21), was significantly less in CD3/28 beads activated cells at day 10 after stimulation (Fig. 1A). Using CFSE, we observed a trend of increased proliferation in T cells stimulated with CD3/28 beads, which was significantly different from cells that received no activation stimulus (Fig. 1B). Besides this, there was no difference in the ability of CD3/28 antibody or CD3/28 beads activated T cells to get transduced and express CARs (Fig. 1C). CAR-T cells activated with CD3/28 beads produced significantly higher levels of IL2 upon antigen-specific stimulation. Nonetheless, antigen-specific IFNγ secretion remained unaffected (Fig. 1D and E). These findings indicate reduced senescence attributed to lesser frequency of $CD57^+$ cells and higher proliferation and expansion potential due to increased frequencies of $Ki67^{bright}$ cells and, further, higher levels of IL2 production by CAR-T cells generated after activation with CD3/28 beads. Thus, we used CD3/28 beads to produce redirected T cells for further experiments.

Deletion of Lck binding domain in CD28 costimulatory moiety provides an activated cell-like gene expression profile in redirected T cells upon antigen encounter. FAP-specific (F19) and control (T1)-redirected T cells with the different costimulations CD28/CD3ζ, Δ-CD28/CD3ζ, and 4-1BB/CD3ζ (Supplementary Fig. S1A) were stimulated with FAP. First, we were interested to identify and compare [fold change (Log2FC)] differentially regulated genes in antigen-specific over control CAR-T cells: F19-CD28/CD3ζ over T1-CD28/CD3ζ, F19-Δ-CD28/CD3ζ over T1-Δ-CD28/CD3ζ and F19-4-1BB/CD3ζ over T1-4-1BB/CD3ζ (Supplementary Fig. S2A) to identify differences in costimulation, which could endow CAR-T cells with improved tumor targeting properties, ideal survival and efficacy. Δ-CD28/CD3ζ costimulation resulted in higher expression of cell cycle genes, indicating enhanced proliferation in an antigen-specific manner (Fig. 2Ai);

Downloaded from http://aacrjournals.org/clincancerres/article-pdf/24/16/3981/2045305/3981.pdf by guest on 27 August 2022

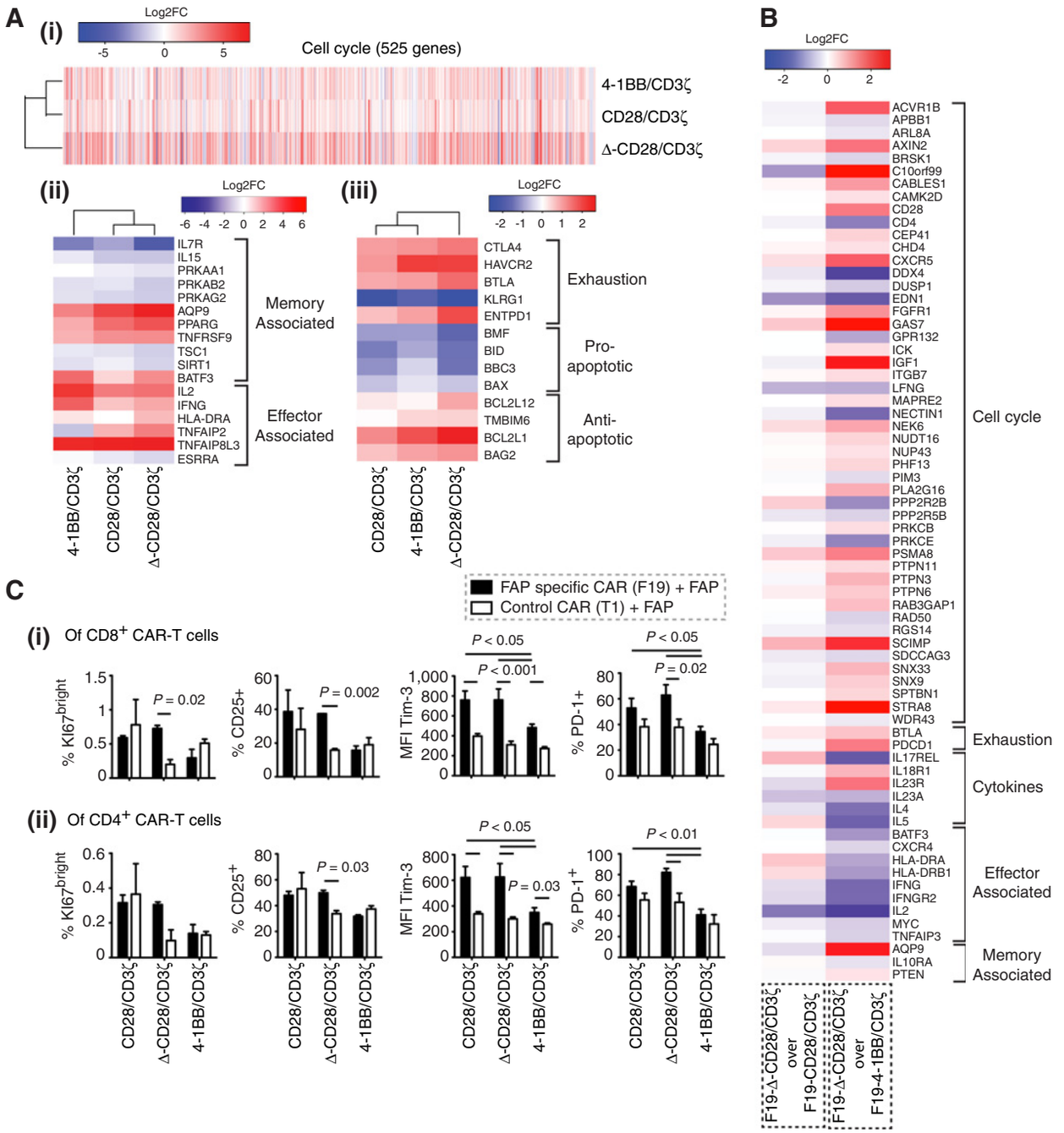

Figure 2.

Transcriptome profiling of redirected T cells and validation of phenotypic markers. RNA sequencing was performed using 3 biological replicates. **A,** Differential expression analysis indicating log fold change (Log2FC) in gene expression of FAP-specific CAR$^+$CD8$^+$ cells over control CAR$^+$CD8$^+$ cells, after stimulation with FAP; CD28/CD3ζ (F19-CD28/CD3ζ over T1-CD28/CD3ζ), Δ-CD28/CD3z (F19-Δ-CD28/CD3ζ over T1-Δ-CD28/CD3ζ) and 4-1BB/CD3ζ (F19-4-1BB/CD3ζ over T1-4-1BB/CD3ζ). Heat maps show differentially regulated genes in (i) cell-cycle pathways (525 genes, enlisted in Supplementary Table S1); (ii) effector or memory phenotype in T cells; and (iii) exhaustion and apoptosis. Color key corresponding to each heat map is presented on the top right corner. Color codes represent Log2FC. **B,** Heatmap showing log fold change (Log2FC) of differentially regulated genes in FAP-specific CARs after antigen stimulation; F19-Δ-CD28/CD3ζ over F19-CD28/CD3ζ and F19-Δ-CD28/CD3ζ over F19-4-1BB/CD3ζ. **C,** Expression of proliferation marker (Ki67), activation marker (CD25), and immune-checkpoint markers (PD-1 and Tim-3) was analyzed by FACS in FAP-specific CAR-T cells (F19-CD28/CD3ζ, F19-Δ-CD28/CD3ζ, and F19-4-1BB/CD3ζ) and control CAR-T cells (T1-CD28/CD3ζ, T1-Δ-CD28/CD3ζ, and T1-4-1BB/CD3ζ) after 6 days of stimulation with antigen (FAP), by comparing the frequencies (%) of Ki67^{bright}, CD25$^+$, and PD-1$^+$ CAR-T cells and median fluorescence intensity of Tim-3 on CAR-T cells of CD8$^+$ (i) or CD4$^+$ (ii) lineage. Representative plots from one experiment with two leucocyte concentrate donors is shown ($n = 2$). Data, mean ± SEM. Statistics is done using unpaired t test, and P values are indicated.

Downloaded from http://aacrjournals.org/clincancerres/article-pdf/24/16/3981/2045305/3981.pdf by guest on 27 August 2022

genes listed in Supplementary Table S1). T cells undergo dynamic metabolic changes during an immune response, which can decide their differentiation and fate (22). We observed that the Δ-CD28/CD3ζ costimulation resulted in relatively increased expression of genes that control cell metabolism such as glycolysis, fatty acid oxidation, and oxidative phosphorylation (Supplementary Fig. S2C). Consistent with this observation, the plasma membrane transporters which play a predominant role in cell metabolism (22) were most distinctly regulated in response to Δ-CD28/CD3ζ costimulation (Supplementary Fig. S2B). We additionally considered key signature markers that distinguish effector T cells from memory T cells. The expression of genes such as IL7R, IL15, AMPK (PRKAA1, PRKAB2 and PRKAG2), TSC1 (negative regulator of mTOR), and SIRT1, which provide a more memory like T-cell phenotype, was increasingly reduced in Δ-CD28/CD3ζ costimulation (Fig. 2Aii). Activation and proliferation of effector T cells are often accompanied by increased levels of inhibitory receptors (20). We found that although Δ-CD28/CD3ζ costimulation resulted in enhanced expression of these receptors, for example, CTLA4, BTLA, ENTPD1 (CD39), and HAVCR2 (Tim-3), it also demonstrated reduced expression of preapoptotic genes and increased expression of antiapoptotic genes (Fig. 2Aiii). Besides, we observed enhanced upregulation of positive and downregulation of negative regulators of autophagy in redirected T cells with Δ-CD28/CD3ζ costimulation (Supplementary Fig. S2D). Albeit the exact relation between autophagy and apoptosis is controversial, research evidence indicates that autophagy can promote T-cell survival by negatively impacting cell death and plays a role in memory formation (23, 24). Overall, our sequencing data indicated a distinct genetic signature consistent with highly proliferating, actively metabolizing, and a terminally differentiated cell-like biology of redirected T cells in response to Δ-CD28/CD3ζ costimulation. To further reveal the specific transcriptional response to Δ-CD28/CD3ζ CAR activation, we additionally compared the transcriptome of FAP specific Δ-CD28/CD3ζ CAR expressing T cells after antigen stimulation with the other two FAP specific CARs (F19-Δ-CD28/CD3ζ over F19-CD28/CD3ζ and F19-Δ-CD28/CD3ζ over F19-4-1BB/CD3ζ). Log2FC of genes identified before and related to cell cycle, cytokines, effector, or memory phenotype in T cells was analyzed (Fig. 2B). Primarily cell-cycle genes were higher expressed in Δ-CD28/CD3ζ CAR expressing T cells after antigen encounter in comparison with the 4-1BB/CD3ζ CAR, while these were already constitutively expressed by CD28/CD3ζ CAR carrying T cells without antigen encounter. Further, to validate our findings at the protein level, we analyzed the expression of Ki67 (proliferation marker), CD25 (activation marker), PD-1 and Tim-3 (activation/exhaustion markers) on FAP-specific (F19-CD28/CD3ζ, F19-Δ-CD28/CD3ζ, and F19-4-1BB/CD3ζ), and control (T1-CD28/CD3ζ, T1-Δ-CD28/CD3ζ, and T1-4-1BB/CD3ζ) CAR-T cells after 6 days of stimulation with FAP. We observed that proliferation and activation was increased in an antigen specific manner in response to Δ-CD28/CD3ζ than CD28/CD3ζ or 4-1BB/CD3ζ costimulations, as indicated by higher frequencies of $Ki67^{bright}$ and $CD25^+$ cells in F19-Δ-CD28/CD3ζ over T1–Δ-CD28/CD3ζ CAR-T cells of $CD8^+$ or $CD4^+$ T-cell lineages (Fig. 2C). In addition to this, the frequency of PD-1^+ cells was antigen specifically enhanced only upon Δ-CD28/CD3ζ costimulation, while Tim-3 expression was consistently augmented in FAP-specific CD28/CD3ζ, Δ-CD28/CD3ζ, and 4-1BB/CD3ζ CARs over their respective controls. There were no remarkable differences observed between FAP-specific CD28/CD3ζ or Δ-CD28/CD3ζ CAR-T cells, besides both of them being significantly distinct from 4-1BB/CD3ζ CAR in terms of expression of activation/exhaustion markers, PD-1 and Tim-3 (Fig. 2C). There were no differences in the expression of apoptotic markers, Bcl-2 (antiapoptotic) and Bax (proapoptotic), at the protein level (Supplementary Fig. S2E). CAR-T cells demonstrated, in general, a more central memory and effector memory like phenotype compared with nontransduced T cells, irrespective of costimulatory signal conferred upon antigen binding (Supplementary Fig. S1B).

Thus, we confirm that antigen-specific Δ-CD28 costimulation provided an exceedingly activated cell-like profile to redirected T cells, as demonstrated by enhanced frequencies of $CD25^+$, $Ki67^{bright}$, and PD-1^+ redirected cells along with increased Tim-3 expression. This phenotype was already displayed in part without antigen stimulation by CD28/CD3ζ CAR-expressing T cells and never to the same extent achieved by 4-1BB/CD3ζ CAR carrying T cells even after antigen stimulation.

Aberrant Lck signaling through the CD28 CAR increases the antigen-specific proliferation of redirected T cells. Next, we investigated the impact of different costimulations on proliferation and efficacy of redirected T cells *in vitro*. Over multiple experiments with several donors ($n = 8$), we observed that CD28/CD3ζ CAR-T cells proliferated unspecifically. In contrast, the Δ-CD28/CD3ζ and 4-1BB/CD3ζ CAR-T cells proliferated equally well in a highly antigen-specific manner (Fig. 3A). Additionally, we observed that the $CD8^+$ CAR-T cells demonstrated significantly higher nonspecific proliferation compared with $CD4^+$ CAR-T cells (Supplementary Fig. S1C). Notably, all three costimulatory CAR constructs demonstrated antigen-specific antitumor cytotoxicity at different E:T ratios (Fig. 3B). Yet, the 4-1BB/CD3ζ CAR showed the least tumor cell lysis which was significantly different from the Δ-CD28/CD3ζ CAR. In addition to this, the frequency of IL2 and IFNγ producing $CD4^+$ and $CD8^+$ CAR-T cells was elevated upon cognate antigen recognition (Fig. 3C and D). Likewise, all the three CAR constructs exhibited antigen-specific IFNγ and IL2 release (Fig. 3E). Even though we observed higher frequency of IL2 producing cells in the 4-1BB/CD3ζ group (Fig. 3C), the amount of IL2 secreted by these cells was very limited (Fig. 3E). The reduced IL2 release by the Δ-CD28/CD3ζ compared with CD28/CD3ζ CAR-T cells has already been reported before (11) and is a consequence of the missing lck signal. However, due to its antigen specificity, the elevated IL2 production by CD28/CD3ζ CAR-T cells can only partially explain the observed antigen-unspecific proliferation. Besides, Δ-CD28/CD3ζ CAR-T cells revealed maximum antigen-specific IFNγ release (Fig. 3E). Thus, our data demonstrate that T cells redirected with Δ-CD28/CD3ζ show less antigen-independent proliferation with similar antigen-specific proliferation, similar killing to CD28, and enhanced IFNγ, but reduced IL2 release.

Lck lacking CD28 CAR-T cells show improved tumor control in combination with PD-1 blockade in tumor-bearing humanized mice. We aimed to study the survival and efficacy of redirected T cells in a humanized mouse model (huNSG). After comparing HFL and leukapheresis products as a source for preparing humanized mice, we chose HFL-derived $CD34^+$ cells to reconstitute NSG mice due to significantly higher levels of human immune cell engraftment in the peripheral blood (Supplementary Fig. S4B). We found that a very high frequency (~90%) of $CD34^+$ HPCs derived from

Downloaded from http://aacrjournals.org/clincancerres/article-pdf/24/16/3981/2045305/3981.pdf by guest on 27 August 2022

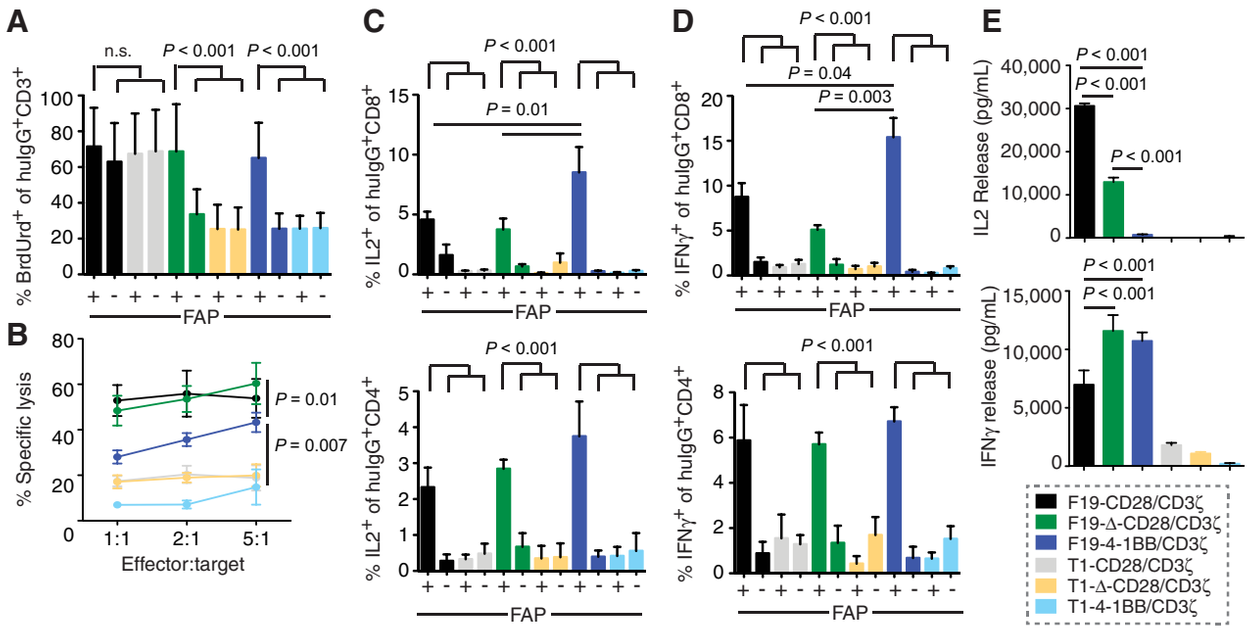

Figure 3.

In vitro functional characterization of redirected T cells with different costimulations. CD3$^+$ cells obtained from buffy donors were transduced to express FAP-specific CARs (F19-CD28/CD3ζ, F19-Δ-CD28/CD3ζ, and F19-4-1BB/CD3ζ) or control CARs (T1-CD28/CD3ζ, T1-Δ-CD28/CD3ζ, and T1-4-1BB/CD3ζ). **A,** Proliferation was compared by culturing CAR transduced cells in BrdU supplemented medium and stimulating with (+) or without (−) antigen (FAP). Frequency of proliferating cells was determined by first gating on hulgG$^+$ (CAR$^+$) cells followed by further selecting BrdU$^+$ cells. Pooled data from eight buffy donors ($n = 4$) are shown. Statistics is done using one-way ANOVA with Tukey's posttest for multiple comparison. **B,** CD3$^+$ CAR-T cells were cocultured with HT1080FAP tumor cells at specified E:T ratios and tumor cell lysis was measured. Intracellular staining was performed to measure the frequency (%) of IL2 (**C**) and IFNγ (**D**) producing CAR-T cells of CD8 (top) or CD4 (bottom) lineage in response to antigen-specific stimulation (+) or no stimulation (−) with FAP. **E,** Cytokines IL2 (top) and IFNγ (bottom) quantified by ELISA in supernatant from cocultures of CD3$^+$ CAR-T cells with tumor cells. Representative data from one experiment with two buffy donors are shown ($n = 4$). *P* value is calculated using unpaired *t* test. Data, mean ± SEM.

leukapheresis coexpressed CD38 (Supplementary Fig. S4C), which is a marker for more differentiated progenitor cells, thereby correlating with the poor multipotency of these cells.

To test survival of redirected T cells in humanized mice, we generated CAR-transduced T cells using splenocytes from humanized mice and injected them into recipient mice that were reconstituted from the autologous HPC donor (Fig. 4A). After adoptive transfer of redirected T cells and serial blood draws (Fig. 4B), CAR-T cells could be detected in the peripheral blood with almost no significant differences between the groups. Up to at least 44 days, redirected T cells persisted in the blood of huNSG without any antigenic stimulus (Fig. 4C and D). At day 44, we found these cells predominantly in the blood and in highest frequency of huNSG mice belonging to the 4-1BB/CD3ζ group (75% mice) compared with CD28/CD3ζ (25% mice) or Δ-CD28/CD3ζ (40% mice) groups. In addition, we found CD28/CD3ζ-redirected T cells in the liver, spleen, and bone marrow of 50%, 25%, and 50% of huNSG mice, respectively. Δ-CD28/CD3ζ-redirected T cells were observed in the bone marrow of 40% huNSG mice and 4-1BB/CD3ζ CAR-T cells in the liver of 25% of huNSG mice (Fig. 4E).

After confirming the survival of redirected T cells, we investigated their impact on tumor development in huNSG mice. We injected human fibrosarcoma cells expressing FAP (HT1080FAP) in huNSG (Fig. 5A). Prior to tumor inoculation, the expression of FAP and PD-L1 was confirmed by flow cytometry (Supplementary Fig. S3A). Ninety-six percent of HT1080FAP tumor cells coexpressed FAP and PD-L1. The HT1080FAP tumor cell line is xenogeneic to the murine host and allogeneic to the reconstituted human immune compartment of the huNSG. To negate the possibility of the reconstituted human immune compartment affecting the tumor development (allogenicity of the tumor cell line toward the host immune cells), we examined the correlation of reconstitution frequency (% CD45$^+$ and % CD3$^+$ cells in blood) in huNSG with tumor development (after tumor inoculation and prior to injecting redirected T cells). We found that tumor take in huNSG mice was not significantly affected by the level of reconstitution (Supplementary Fig. S4D). The tumor-bearing humanized mice were similarly distributed into different experimental groups based on reconstitution in blood (% CD45$^+$) and tumor load (Supplementary Fig. S4E), prior to adoptive transfer of redirected T cells. As described previously, we injected tumor in the peritoneal cavity. Due to the strong expression of PD-L1 on the tumor cells (Supplementary Fig. S3A) and a high frequency of redirected T cells expressing PD-1 (Fig. 2C), the model allows for the testing of PD-1 blockade with T cells expressing different CAR constructs. Before transfer, there was no *in vitro* effect of PD-1 blockade with regard to proliferation and antigen-specific cell killing by redirected T cells (Supplementary Fig. S3B and S3C). After implantation of the tumor cells, functionally tested (*in vitro*)-redirected T cells (Fig. 5B–D) were transferred in the peritoneal cavity (in proximity to tumor), and

Downloaded from http://aacrjournals.org/clincancerres/article-pdf/24/16/3981/2045305/3981.pdf by guest on 27 August 2022

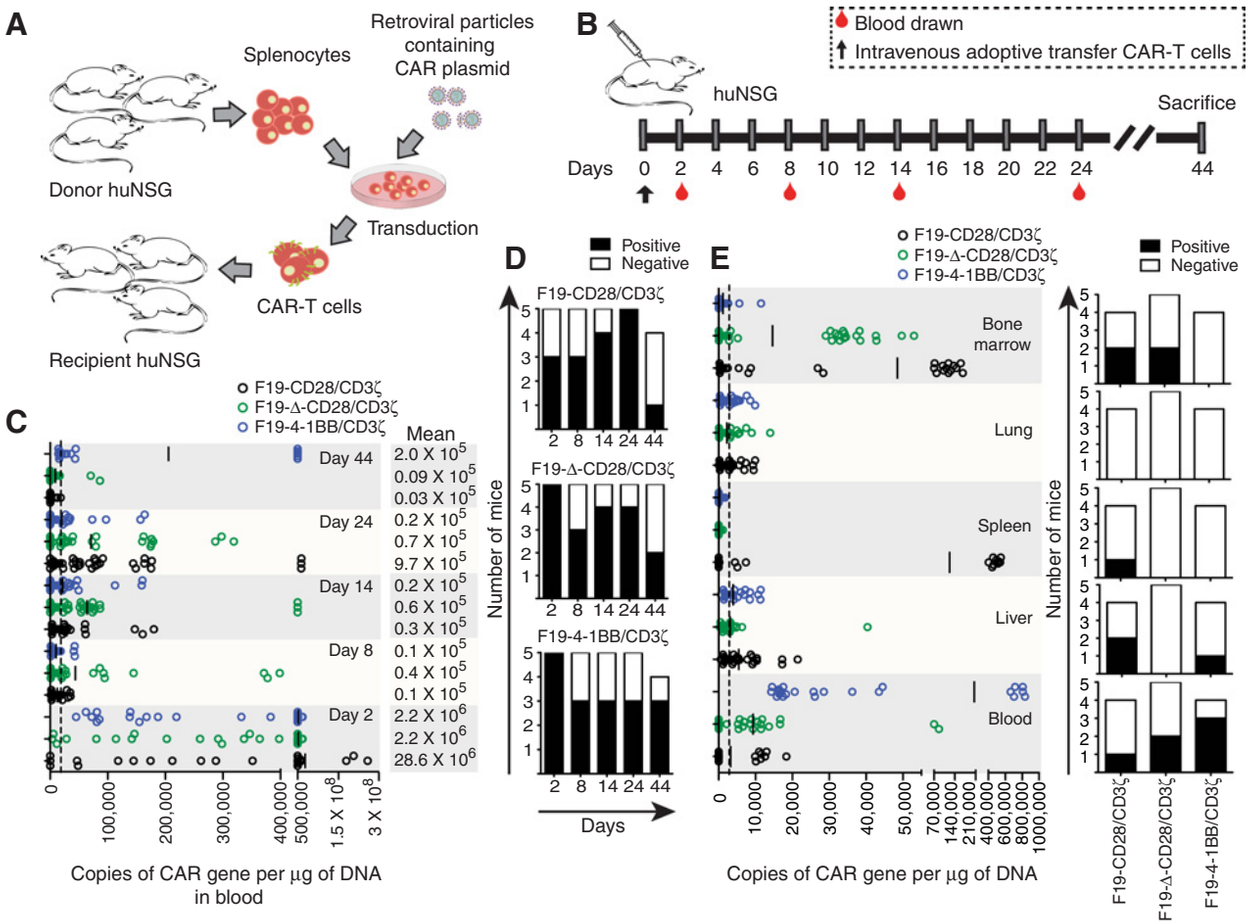

Figure 4.
Survival of redirected T cells in humanized mice. **A,** Splenocytes were harvested from donor humanized NSG (huNSG) mice and transduced to express FAP-specific CARs with different costimulations (F19-CD28/CD3ζ, F19-Δ-CD28/CD3ζ, and F19-4-1BB/CD3ζ). Redirected T cells were then injected into recipient huNSG mice. **B,** Time line of the adoptive transfer experiment is shown. Redirected T cells were injected intravenously at day 0. Blood was drawn at days 2, 8, 14, 24, and 44 after adoptive transfer. Mice were sacrificed at day 44, and organs were harvested. **C,** Copies of CAR gene per µg of DNA in blood at days 2, 8, 14, 24, and 44 as quantified by qPCR. Mean CAR copies corresponding to each group and time point are indicated (−) and mentioned (right). Each circle represents one qPCR replicate (∼6 replicates per mouse). Dashed line indicates minimum detection threshold. **D,** Number of mice (Y-axis) that showed positive CAR copies in the blood at specified time points (X-axis) in the F19-CD28/CD3ζ (top), F19-Δ-CD28/CD3ζ (middle), and F19-4-1BB/CD3ζ group (bottom). **E,** Copies of CAR gene per µg of DNA in blood, liver, spleen, lungs, and BM of harvested mice at day 44. Each circle illustrates one qPCR replicate (∼6 replicates per mouse). Mean values are marked (−). Right, Number of mice (Y-axis) that showed positive CAR copies in corresponding organs in each group (X-axis). Representative data from one experiment with five mice per group are shown ($n = 3$).

PD-1–blocking antibody was administered. Surprisingly, only redirected T cells expressing the F19-Δ-CD28/CD3ζ CAR-induced significantly attenuated tumor growth (Fig. 5F) and provided an improved survival of mice (Fig. 5G). FAP expression was confirmed on tumors harvested from mice by immunohistochemistry (Fig. 5E). No redirected T cells could be measured in the peripheral blood (Fig. 5H; Supplementary Fig. S5A). Persistence of redirected T cells could be identified in the tumor-infiltrating lymphocytes (TIL) and peritoneal lavage (Fig. 5H). Interestingly, persistence was significantly enhanced in T cells redirected by the 4-1BB/CD3ζ CAR but without antitumor efficacy. Nevertheless, only the number of redirected T cell with Δ-CD28 costimulation showed a significant inverse correlation with tumor development (Fig. 5I; Supplementary Fig. S5B). Finally, there was no statistically significant difference in frequency of Treg-infiltrating tumors between the different CAR groups (Supplementary Fig. S5C), suggesting no prominent role of regulatory T cells for the stronger therapeutic effect mediated by the Δ-CD28/CD3ζ CAR with PD-1 blockade.

First-in-man adoptive transfer of lck lacking CD28 CAR showed persistence of redirected T cells up to 21 days. Based on our initial data, we designed a first-in-man clinical protocol (9) for the treatment of patients with MPM with FAP-specific redirected T cells and to implement FAP-specific redirected T cells as a platform for combination therapies as exemplarily tested in the previously described experiments. In this clinical trial, we aimed to use a new application method for the administration of redirected T cells supported by our experience from mouse models. Redirected T cells were injected in proximity to the malignant cells directly into

Downloaded from http://aacrjournals.org/clincancerres/article-pdf/24/16/3981/2045305/3981.pdf by guest on 27 August 2022

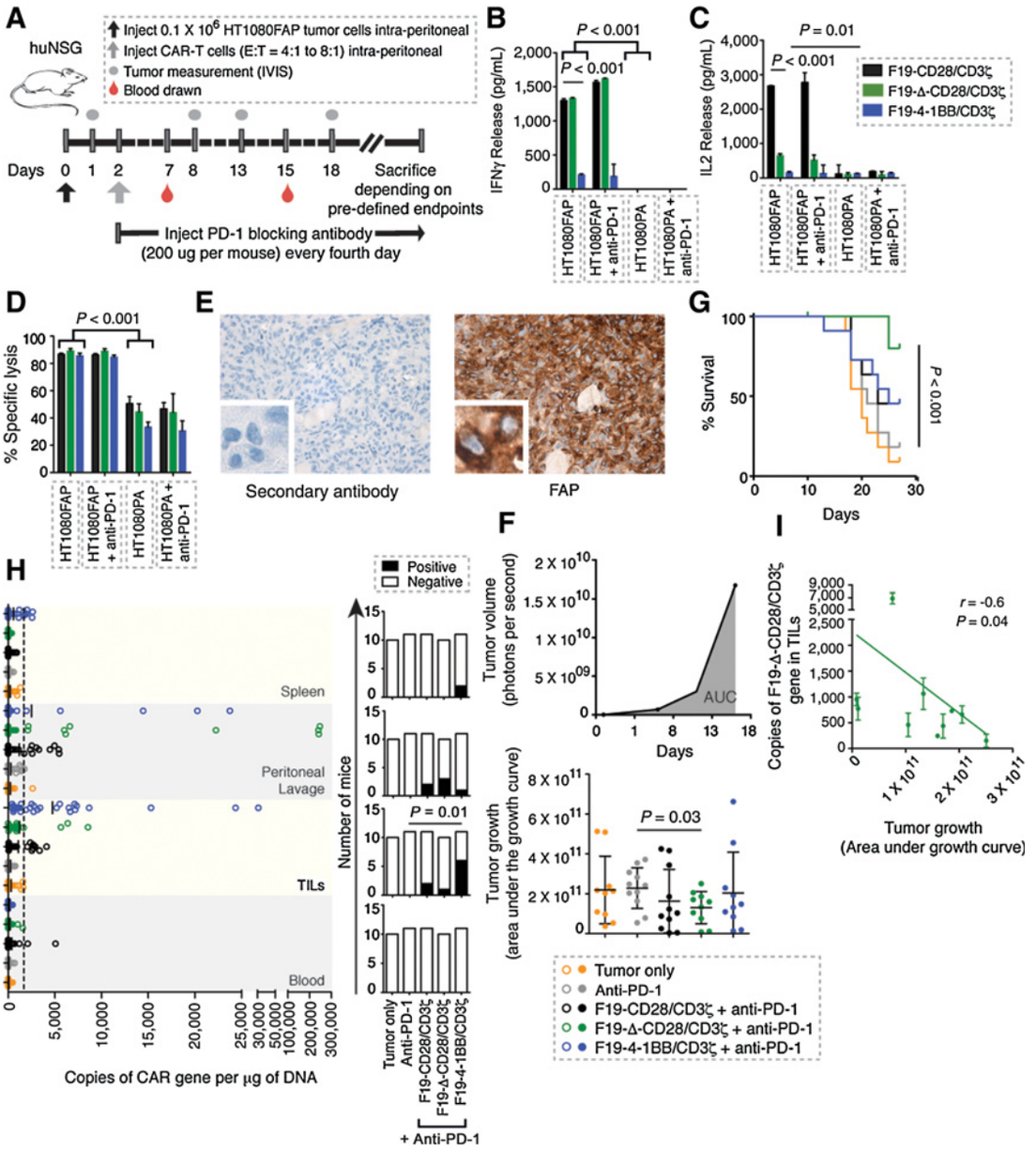

Figure 5.

Redirected T cells with Δ-CD28 costimulation show better tumor control in humanized mice and persistence in tumor-infiltrating lymphocytes (TIL) and peritoneal lavage (PL). **A,** Timeline of adoptive transfer. HT1080FAP cells were injected i.p. in huNSG mice at day 0, followed by measuring tumor in IVIS at day 1. After grouping mice based on tumor development, redirected T cells produced from donor matched littermates were injected at day 2 at E:T = 4:1 to 8:1. Blood was drawn on days 7, 15, and at the time of sacrifice. Tumor measurements were performed at days 1, 8, 13, and 18 after tumor injection. Mice were sacrificed based on predefined endpoints, and the experiment was terminated at day 27. Starting from day 2, mice received PD-1–blocking antibody every fourth day. FAP-specific redirected T cells produced from donor matched littermates of huNSG were cocultivated with tumor cells expressing FAP (HT1080FAP) or no FAP (HT1080PA) with or without PD-1–blocking antibody (anti–PD-1) and (**B**) IFNγ and (**C**) IL2 release in supernatants and (**D**) *in vitro* tumor cell lysis is shown ($n = 2$). *P* value calculated using an unpaired *t* test. **E,** Representative tumor section of a mouse stained for FAP (right) or secondary antibody control (left); original magnification, 400×. **F,** Tumor volume measured *in vivo* as photons per second (in IVIS) at days 1, 8, 13, and 18 was plotted and area under the tumor growth curve (AUC) was calculated for each mouse. Top, Representative plot from one mouse with AUC highlighted in gray. Bottom, Comparison of tumor growth measured as AUC. Each dot represents the AUC of one mouse. Data, mean ± SD. *P* value is calculated using Mann–Whitney test. **G,** Percentage of survival of mice is indicated by a Kaplan–Meier curve. *P* value is calculated using the log-rank test. **H,** Copies of CAR gene per μg of DNA was quantified by qPCR in blood, TILs, PL, and spleen of harvested mice (left). Each circle indicates one qPCR replicate (total 3 replicates per mouse). Dashed line indicates minimum detection threshold. Right, Number of mice (Y-axis) from each group (X-axis) that showed positive CAR copies in the corresponding organ. *P* value is calculated using the Fisher exact test. **I,** Correlation of copies of the F19-Δ-CD28/CD3ζ gene in TILs with tumor growth (area under the curve). Data, mean ± SEM. Spearman correlation coefficient (*r*) and *P* value is mentioned. Each dot is one mouse ($n = 11$). Error bars, Variation between qPCR replicates. Cumulative data from 3 cohorts of mice in two independent experiments is shown (total mice per group = 11).

Downloaded from http://aacrjournals.org/clincancerres/article-pdf/24/16/3981/2045305/3981.pdf by guest on 27 August 2022

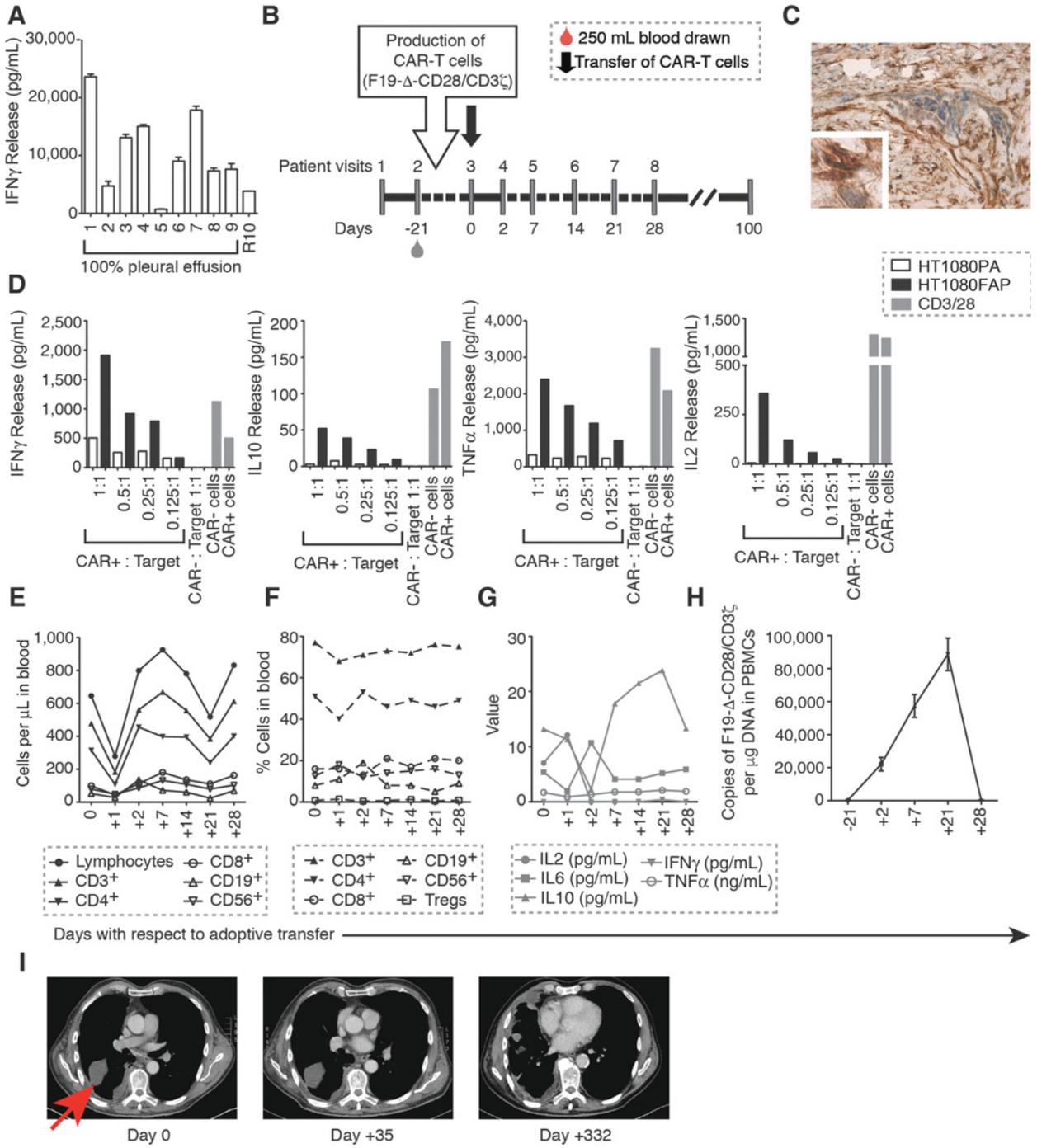

Figure 6.

First-in-man adoptive transfer of lck lacking CD28 CAR showed persistence of redirected T cells up to 21 days in peripheral blood. **A,** F19-Δ-CD28/CD3ζ-redirected T cells were incubated with HT1080FAP target cell in pleural effusions from different donors (1–9) or culture media (R10) and IFNγ release was measured by ELISA. **B,** Time schedule of the clinical phase I trial; **C,** biopsy of patient, 6 months after adoptive transfer, stained for FAP (original magnification, 400×). **D,** GMP produced, redirected FAP-specific T cells were tested *in vitro* before transfer in different effector to target ratios and cytokines were measured. "CAR-" indicates untransduced T cells. **E,** Absolute counts of leukocyte subsets; **F,** percentages of leukocyte subsets; **G,** cytokine levels measured in the peripheral blood; and **H,** copy numbers of the CAR (F19-Δ-CD28/CD3ζ) gene in the peripheral blood measured in relation to peripheral blood mononuclear cell (PBMC) DNA amount (per µg). **I,** CT scan of lungs on different time points with respect to adoptive transfer. → indicates the pleural effusion, in which the redirected T cells were injected.

Downloaded from http://aacrjournals.org/clincancerres/article-pdf/24/16/3981/2045305/3981.pdf by guest on 27 August 2022

the pleural infusion (Fig. 6I). To better characterize the injection site, pleural effusions of different patients with MPM were analyzed as the first step. Some MPM pleural effusions showed prominent levels of TGFβ, IL10, and VEGF, suggesting an immune-suppressive microenvironment (Supplementary Fig. S6). However, these pleural effusions did not block in general the antigen-specific release of IFNγ when compared with cell culture supernatant (Fig. 6A). The first patient was treated 21 days after collection of autologous PBMCs and GMP redirection of his T cells by the F19-Δ-CD28/CD3ζ CAR against FAP (Fig. 6B). At the day of transfer, the patient's redirected T cells were also tested *ex vivo* (Fig. 6D). These cells showed antigen-specific release of IFNγ, IL2, IL10, and TNFα. A biopsy at 6 months after adoptive transfer confirmed FAP expression mainly in the stroma (Fig. 6C). Next, the lymphocyte counts, cytokines, and the CAR persistence was evaluated in the peripheral blood according to the study protocol. Initially, lymphocyte counts and cytokines levels (IFNγ, IL2, IL6, IL10, and TNFα) dropped, followed by an increase of IL10 at later time points (Fig. 6E–G). Most interestingly, we observed F19-Δ-CD28/CD3ζ CAR-T cell expansion, which peaked in the peripheral blood at day 21 after infusion (Fig. 6H). The first patient of the clinical trial showed stable disease for about 1 year after adoptive transfer (Fig. 6I). At progression, he then received PD-1 blockade for 6 months. Thus, the stable disease might have been supported by the CAR-T cell therapy.

Discussion

We previously investigated the therapeutic effect of FAP-specific, redirected T cells as an option for treatment of MPM (9, 11). Functional T cells expressing anti-FAP CARs at high level could be generated by standard procedures and these redirected T cells showed antigen-specific activity (11). The most recent research in the field of redirected T cells analyzes a multitude of different CAR constructs, of which CARs with CD28 or 4-1BB costimulation are most frequently used. This led us to question, which costimulation through the CAR should be combined with FAP-specificity for MPM treatment.

We developed a novel humanized mouse model with autologous redirected T cells, thereby avoiding development of GvHD and allogeneic rejection of the transferred, redirected T cells. In this model, the tumor cell line used is allogeneic to the reconstituted immune compartment of humanized mice. However, even a small number of allogeneic tumor cells (0.1×10^6) resulted in a reliable tumor take. This result is even more surprising because it is estimated that the humanized T-cell repertoire contains about 5% alloreactive T cells, which had no effect on tumor take (25). Therefore, the effects of redirected T cells do not seem to be enhanced by allogeneic endogenous T cells and speaks to the low immunogenicity of the tumor cell line.

We observed improved persistence of autologous redirected T cells in humanized mice, considering previously observed survival of up to 3 weeks in NSG mice (13). As expected, the 4-1BB/CD3ζ CAR performed best with regard to persistence until day 44 in the peripheral blood of humanized mice. Multiple reasons could be responsible for this observation. Humanized mice have low levels of human cytokines, which are essential to support transferred T cells. *In vitro*–redirected T cells are dependent on continuous support from cytokines like IL2, IL7, and IL15. Some animal models tried to overcome this limitation by expressing human cytokines, like IL7 transgenic NSG mice and, therefore, are potential candidate models to further improve the herein presented model (26). An alternative explanation for the rather short persistence in mice without human immune system reconstitution could be that T cells are not supported without antigen stimulation and/or HLA stimulation (27). Nevertheless, even in the first patient—who served as the ultimate host for his autologous redirected T cells—the CAR-T cells expanded, but persisted no longer than 21 days at detectable levels in the peripheral blood.

This rather short persistence in humanized mice and man may also be explained by the state of the T cells. Due to the process by which redirected T cells are produced, the main phenotypes of redirected T cells are effector memory or effector phenotype (13). When comparing T cells expressing the Δ-CD28/CD3ζ, CD28/CD3ζ, and 4-1BB/CD3ζ CAR, which had the same phenotype after production, differences could be observed regarding gene expression profiles induced by antigen stimulation. Previously, the comparison of the CARs using CD28 or 4-1BB highlighted the different gene expression profile indicating different metabolic programs (28). The authors have shown that CAR-T cells with 4-1BB costimulation developed more readily a central memory phenotype while CD28 costimulation yielded effector memory T cells (28). Noteworthy, in our experiments, the CD28/CD3ζ CAR showed unspecific proliferation. Similar observation of antigen independent signaling through CD28 costimulatory CARs was shown before (29) and attributed to certain framework regions in the scFv fragments. Another study showed that CD28 CARs may mediate constitutive expression of IL2 and proliferation of T cells (30). Our data indicate that lck deletion results in improved antigen-specific proliferation, which might be in part attributed to less constitutive IL2 secretion and therefore less tonic signaling. In addition, the Δ-CD28/CD3ζ CAR led to a new and distinct supraphysiologic gene expression profile in activated $CD8^+$ T cells. It induced the expression of gene programs of effector and memory T cells: glycolysis, exhaustion (effector programs), and fatty acid oxidation and antiapoptosis (memory programs). This, in theory, advantageous combination did not result in prolonged persistence.

Nevertheless, *in vivo* functionality of the redirected T cells could be tested with some encouraging results. Only the combination of Δ-CD28/CD3ζ CAR redirected T cells with PD-1 blockade resulted in statistically significant tumor control. In contrast, it was shown recently that redirected T cells with CD28 costimulation showed increased *in vivo* functionality in a mesothelioma model using immune-compromised mice (31). We speculate that the different results are, in part, attributable to interactions of the humanized immune system and the redirected T cells. One potential argument could be clonal competition for cytokines, and another, increased immune suppression by parts of humanized immune system in the tumor microenvironment (e.g., regulatory T cells).

Previously, it has been shown that regional delivery of CAR-T cells vastly outperforms systemically infused T cells in mouse models (32). Thus, our line of experimentation and the early clinical trial were focused on the local injection of redirected T cells in body cavities harboring the tumor cells (intraperitoneal model system in mice and pleural effusion in the clinical trial). Other clinical trials have also followed this approach to overcome the issue of T-cell trafficking (33). Our experimental data indicate that redirected T cells injected into a tumor-bearing cavity encounter the tumor and cause tumor control.

Downloaded from http://aacrjournals.org/clincancerres/article-pdf/24/16/3981/2045305/3981.pdf by guest on 27 August 2022

Overall, we describe here a first humanized mouse model for autologous redirected T cells. We showed that adoptive transfer of FAP-specific redirected T cells with a special CAR lacking lck signaling through CD28 costimulation, in combination with PD-1 blockade, induced transient tumor control. Additionally, we took this approach from bench to bedside and demonstrate the first clinical feasibility of this novel therapeutic concept. Concomitant combinations of PD-1 blockade and FAP-specific CAR-T cells should be clinically explored in the future.

Disclosure of Potential Conflicts of Interest

No potential conflicts of interest were disclosed.

Authors' Contributions

Conception and design: P. Gulati, C. Renner, C. Münz, U. Petrausch
Development of methodology: P. Gulati, P. Schuberth, M. Pruschy, A. Tabor, U. Petrausch
Acquisition of data (provided animals, acquired and managed patients, provided facilities, etc.): P. Gulati, J. Rühl, M. Pircher, K.J. Nytko, M. Pruschy, M. Haefner, A. Soltermann, W. Jungraithmayr, M. Eisenring, T. Winder, P. Samaras, A. Tabor, R. Stupp, C. Renner
Analysis and interpretation of data (e.g., statistical analysis, biostatistics, computational analysis): P. Gulati, A. Kannan, M. Pruschy, A. Soltermann, P. Samaras, C. Renner, U. Petrausch
Writing, review, and/or revision of the manuscript: P. Gulati, S. Jensen, A. Soltermann, T. Winder, P. Samaras, R. Stupp, W. Weder, C. Renner, C. Münz, U. Petrausch
Administrative, technical, or material support (i.e., reporting or organizing data, constructing databases): P. Gulati, S. Sulser, A. Soltermann, W. Jungraithmayr, T. Winder, R. Stenger, R. Stupp
Study supervision: C. Renner, C. Münz

Acknowledgments

This work was supported by "Forschungskredit" University of Zurich (grant number 54171101), Swiss Cancer League (grant numbers KFS-3115-02-2013 and KFS-4231-08-2017), "Hoch spezialisierte Medizin" of the Canton Zurich, Swiss Tumor Immunology Institute, and Zurich Cancer League. We thank the first patient and his family for their strong will to support modern therapies in an open and positive manner. We would like to thank Dorothea Greuter, Claudia Bonvin, and Claudia Matter for excellent technical assistance. We thank Hinrich Abken and Markus Chmielewski (University of Cologne, Germany) for the pBullet plasmid. We are indebted to Helga Bachmann for the data management. We further thank George Coukos, Silke Gillessen, Alexander Jetter, and Georg Stüssi for volunteering for the safety board. We would like to thank Uta Henze from the SCRM for the quality control process. We express gratitude to Mark Robinson for his assistance and support in analysis of RNA sequencing data. The phase I study of testing of FAP-redirected T cells in MPM was partly planned and designed at the 12th joint ECCO–AACR–EORTC–ESMO Workshop "Methods in Clinical Cancer Research," Waldhaus Flims, Switzerland, June 19–25, 2010.

The costs of publication of this article were defrayed in part by the payment of page charges. This article must therefore be hereby marked *advertisement* in accordance with 18 U.S.C. Section 1734 solely to indicate this fact.

Received June 23, 2017; revised November 23, 2017; accepted May 2, 2018; published first May 10, 2018.

References

1. Sadelain M, Brentjens R, Rivière I. The basic principles of chimeric antigen receptor design. Cancer Discov 2013;3:388–98.
2. Jackson HJ, Rafiq S, Brentjens RJ. Driving CAR T-cells forward. Nat Rev Clin Oncol 2016;13:370–83.
3. Alcantar-Orozco EM, Gornall H, Baldan V, Hawkins RE, Gilham DE. Potential limitations of the NSG humanized mouse as a model system to optimize engineered human T cell therapy for cancer. Hum Gene Ther Methods 2013;24:310–20.
4. Gaska JM, Ploss A. Study of viral pathogenesis in humanized mice. Curr Opin Virol 2015;11:14–20.
5. Shultz LD, Brehm MA, Garcia-Martinez JV, Greiner DL. Humanized mice for immune system investigation: progress, promise and challenges. Nat Rev Immunol 2012;12:786–98.
6. Weder W, Opitz I, Stahel R. Multimodality strategies in malignant pleural mesothelioma. Semin Thorac Cardiovasc Surg 2009;21:172–6.
7. Karrison HK, Rose Y-HCT, Straus MA, Sargis R, Seiwert T. Phase II trial of pembrolizumab in patients with malignant mesothelioma (MM): interim analysis volume Vol. 12 J Thoracic Oncol.
8. Quispel-Janssen J, Zago G, Schouten R, Buikhuisen W, Monkhorst K, Thunissen E, et al. A phase II study of nivolumab in malignant pleural mesothelioma (NivoMes): with translational research (TR) biopies. 2017;12:S292–S293.
9. Petrausch U, Schuberth PC, Hagedorn C, Soltermann A, Tomaszek S, Stahel R, et al. Re-directed T cells for the treatment of fibroblast activation protein (FAP)-positive malignant pleural mesothelioma (FAPME-1). BMC Cancer 2012;12:615.
10. Kofler DM, Chmielewski M, Rappl G, Hombach A, Riet T, Schmidt A, et al. CD28 costimulation impairs the efficacy of a redirected t-cell antitumor attack in the presence of regulatory t cells which can be overcome by preventing Lck activation. Mol Ther 2011;19:760–7.
11. Schuberth PC, Hagedorn C, Jensen SM, Gulati P, van den Broek M, Mischo A, et al. Treatment of malignant pleural mesothelioma by fibroblast activation protein-specific re-directed T cells. J Transl Med 2013;11:187.
12. Heller KN, Upshaw J, Seyoum B, Zebroski H, Münz C. Distinct memory $CD4^+$ T-cell subsets mediate immune recognition of Epstein Barr virus nuclear antigen 1 in healthy virus carriers. Blood 2007;109:1138–46.
13. Schuberth PC, Jakka G, Jensen SM, Wadle A, Gautschi F, Haley D, et al. Effector memory and central memory NY-ESO-1-specific re-directed T cells for treatment of multiple myeloma. Gene Ther 2012.
14. Weijtens ME, Willemsen RA, van Krimpen BA, Bolhuis RL. Chimeric scFv/gamma receptor-mediated T-cell lysis of tumor cells is coregulated by adhesion and accessory molecules. Int J Cancer 1998;77:181–7.
15. Hombach A, Hombach AA, Abken H. Adoptive immunotherapy with genetically engineered T cells: modification of the IgG1 Fc`spacer' domain in the extracellular moiety of chimeric antigen receptors avoids 'off-target' activation and unintended initiation of an innate immune response. Gene Ther 2010;17:1206–13.
16. Ferlazzo G, Thomas D, Lin SL, Goodman K, Morandi B, Muller WA, et al. The abundant NK cells in human secondary lymphoid tissues require activation to express killer cell Ig-like receptors and become cytolytic. J Immunol 2004;172:1455–62.
17. Vignali DA. Multiplexed particle-based flow cytometric assays. J Immunol Methods 2000;243:243–55.
18. Strowig T, Chijioke O, Carrega P, Arrey F, Meixlsperger S, Rämer PC, et al. Human NK cells of mice with reconstituted human immune system components require preactivation to acquire functional competence. Blood 2010;116:4158–67.
19. Strowig T, Gurer C, Ploss A, Liu YF, Arrey F, Sashihara J, et al. Priming of protective T cell responses against virus-induced tumors in mice with human immune system components. J Exp Med 2009;206:1423–34.
20. Wei F, Zhong S, Ma Z, Kong H, Medvec A, Ahmed R, et al. Strength of PD-1 signaling differentially affects T-cell effector functions. Proc Natl Acad Sci U S A 2013;110:E2480–9.
21. Brenchley JM, Karandikar NJ, Betts MR, Ambrozak DR, Hill BJ, Crotty LE, et al. Expression of CD57 defines replicative senescence and antigen-induced apoptotic death of CD8+ T cells. Blood 2003;101:2711–20.
22. O'Sullivan D, Pearce EL. Targeting T cell metabolism for therapy. Trends Immunol 2015;36:71–80.
23. Xu X, Araki K, Li S, Han JH, Ye L, Tan WG, et al. Autophagy is essential for effector CD8(+) T cell survival and memory formation. Nat Immunol 2014;15:1152–61.

Downloaded from http://aacrjournals.org/clincancerres/article-pdf/24/16/3981/2045305/3981.pdf by guest on 27 August 2022

24. Kovacs JR, Li C, Yang Q, Li G, Garcia IG, Ju S, et al. Autophagy promotes T-cell survival through degradation of proteins of the cell death machinery. Cell Death Differ 2012;19:144–52.
25. Suchin EJ, Langmuir PB, Palmer E, Sayegh MH, Wells AD, Turka LA. Quantifying the frequency of alloreactive T cells in vivo: new answers to an old question. J Immunol 2001;166:973–81.
26. van Lent AU, Dontje W, Nagasawa M, Siamari R, Bakker AQ, Pouw SM, et al. IL-7 enhances thymic human T cell development in "human immune system" Rag2-/-IL-2Rgammac-/- mice without affecting peripheral T cell homeostasis. J Immunol 2009;183:7645–55.
27. Billerbeck E, Horwitz JA, Labitt RN, Donovan BM, Vega K, Budell WC, et al. Characterization of human antiviral adaptive immune responses during hepatotropic virus infection in HLA-transgenic human immune system mice. J Immunol 2013;191:1753–64.
28. Kawalekar OU, O'Connor RS, Fraietta JA, Guo L, McGettigan SE, Posey AD, et al. Distinct signaling of coreceptors regulates specific metabolism pathways and impacts memory development in CAR T cells. Immunity 2016;44:380–90.
29. Long AH, Haso WM, Shern JF, Wanhainen KM, Murgai M, Ingaramo M, et al. 4–1BB costimulation ameliorates T cell exhaustion induced by tonic signaling of chimeric antigen receptors. Nat Med 2015;21:581–90.
30. Frigault MJ, Lee J, Basil MC, Carpenito C, Motohashi S, Scholler J, et al. Identification of chimeric antigen receptors that mediate constitutive or inducible proliferation of T cells. Cancer Immunol Res 2015;3:356–67.
31. Cherkassky L, Morello A, Villena-Vargas J, Feng Y, Dimitrov DS, Jones DR, et al. Human CAR T cells with cell-intrinsic PD-1 checkpoint blockade resist tumor-mediated inhibition. J Clin Invest 2016;126:3130–44.
32. Adusumilli PS, Cherkassky L, Villena-Vargas J, Colovos C, Servais E, Plotkin J, et al. Regional delivery of mesothelin-targeted CAR T cell therapy generates potent and long-lasting CD4-dependent tumor immunity. Sci Transl Med 2014;6:261ra151.
33. Brown CE, Alizadeh D, Starr R, Weng L, Wagner JR, Naranjo A, et al. Regression of glioblastoma after chimeric antigen receptor T-cell therapy. N Engl J Med 2016;375:2561–9.

Downloaded from http://aacrjournals.org/clincancerres/article-pdf/24/16/3981/2045305/3981.pdf by guest on 27 August 2022